Aerodynamic Characteristics of a Standard Dynamics Model in a Spinning Motion

Article *in* Journal of Aeronautics, Astronautics and Aviation, Series A · June 2022

DOI: 10.6125/JoAAA.202206_54(2).07

5 authors, including:

kung-Ming Chung
National Cheng Kung University
157 PUBLICATIONS **1,314** CITATIONS
SEE PROFILE

Yi-Xuan Huang
National Cheng Kung University
11 PUBLICATIONS **38** CITATIONS
SEE PROFILE

Wei-Han Chen
Georgia Institute of Technology
7 PUBLICATIONS **28** CITATIONS
SEE PROFILE

Journal of Aeronautics, Astronautics and Aviation, Vol. 54, No. 2, pp. 215 – 226 (2022)
DOI: 10.6125/JoAAA.202206_54(2).07

Aerodynamic Characteristics of a Standard Dynamics Model in a Spinning Motion *

K.M. Chung [1] **, Y.X. Huang [2], W.H. Chen [1], Y.T. Liao [3], and J.M. Huang [3]

[1] *Aerospace Science and Technology Research Center, National Cheng Kung University, Tainan, Taiwan*
[2] *Department of Aeronautics and Astronautics, National Cheng Kung University, Tainan, Taiwan, Taiwan*
[3] *Aeronautical Systems Research Division, National Chung-Shan Institute of Science and Technology, Taichung, Taiwan*

ABSTRACT

A rotary balance technique is developed at the Aerospace Science and Technology Research Center (ASTRC) of National Chung Kung University. The aerodynamic characteristics of a standard dynamics model (SDM) with a generic fighter-aircraft shape in a spinning motion are determined for an angle of attack of 0°~30° and a reduced frequency of -0.1~0.1. For a specific angle of attack, a change in the reduced frequency has a minor effect on the coefficients for normal force and pitching moment. The difference between the data and the results from other wind tunnel tests (NASA Ames and FD-09) increases as the angle of attack increases, so the Reynolds number and the compressibility for coefficients of normal force and pitching have an effect. For side force and rolling/yawing moments, the results agree reasonably well, as do the derivatives with respect to the rotational speed.

Keywords: Rotary balance; Standard dynamics model; Spinning

I. INTRODUCTION

Fighter aircraft must maintain maneuverability at high angles of attack. If the aircraft approaches the critical angle of attack (stall angle), a yawing or rolling movement results in a turning force and produces an imbalance in the load on the wings. Autorotation can occur in a helical pattern that is centered in a vertical axis (coning motion) and the stalled aircraft descends rapidly. This is an incipient spin, which is dominated by roll and yaw motions. In the developed stage, the spin frequency (number of rotations per second, Ω) and the radius (distance between the aircraft's center of gravity and the vertical spin axis) stabilizes [1]. There are four different modes of spin, which are defined by the angle of attack, α: steep (α = 20°-30°), moderately steep (α = 30°-45°), moderately flat (α = 45°-65°) and flat (α = 65°-90°) [2]. A spin poses great danger to an aircraft and a pilot and numerous studies predict spin characteristics [3-7].

A spin is a nonlinear phenomenon and is maintained by a balance between the aerodynamic and inertial forces and moments. A aerodynamic modelling involves static aerodynamics (static aerodynamics over a very wide range of α and sideslip angle, β), forced oscillation aerodynamics (oscillating about a given body axis at a fixed frequency and amplitude) and rotary aerodynamics (angular rate or spin frequency) [8-10]. The data is used to determine dynamic stability and for simulations involving an aircraft in a spinning motion [11].

Rotary balance apparatus simulates a steady spinning motion [12-20]. The spinning axis for an aircraft at a specific value for α and β is aligned with the freestream velocity vector. This gives information about the effect of Ω on the aerodynamic forces and the moments that act on an aircraft. The reduced frequency, κ (= Ωb/2V), describes the non-dimensional rotation rate that is experienced by a full-scale aircraft, where b and V are the wing span and the freestream velocity, respectively. Various countries have developed their own rotary balance apparatus for wind tunnel experiments [21]. The maximum value for V and the Reynolds number are 90 m/s and 6×10^6, respectively, and κ has a maximum value of 1.0. The rotary balance apparatus at NASA Ames determines the effect of

* Manuscript received, February 8, 2022, final revision, March 2, 2022
** To whom correspondence should be addressed, E-mail: kmchung@mail.ncku.edu.tw

compressibility in a steady spin mode for a freestream Mach number of 0.6.

This study develops a rotary balance technique at the ASTRC of National Chung Kung University. The aerodynamic measurements use a 5-component force balance. The data for a SDM in a spinning motion is compared with the results of other studies [22, 23] to determine the effect of the Reynolds number and the compressibility.

II. METHODOLOGY

2.1 Low speed wind tunnel and test model

Experiments were conducted in a closed-loop, low-speed wind tunnel at the ASTRC of National Cheng Kung University. There is a honeycomb and five screens upstream of a nozzle (contraction ratio = 9). The constant-area test section is 1.2 m (height) x 1.8 m (width) and it is 2.75 m long. A 450-HP axial-flow fan (Flakt, FAC-6-280-10-12, with a maximum flow rate of 164 m^3/sec, Herne, Germany) provides variable air flow by means of controllable pitch blades using an auxiliary compressor. An inverter (Fuji, FRENIC4600FM5e, Tokyo, Japan) is also used to vary the value of V between 3 m/s and 67 m/s which is determined by the differential pressure between the inlet and the exit of the nozzle using a pressure transducer (GP50, Model 216-C-SZ-CA/LB; range = 0–2.6 kPa; static accuracy = ±0.2%FS, Grand Island, New York). The freestream turbulence intensity is determined to be 0.25%~0.35%.

A SDM that was designed by the National Aeronautical Establishment (NAE), Canada [22, 24] resembles a high-performance aircraft configuration. The model was 3D printed using a DUAL-300 FDM3D printer (Ping, Taichung, Taiwan) which has a net build volume of ∅300mm x H270 mm and a resolution of 0.05 mm per layer and was constructed using Poly Lactic Acid (PLA). The weight is 770 g. As shown in Fig. 1, the SDM has a value for b of 0.343 m and a wing mean aerodynamic chord, l, of 0.129 m. The center of rotation is located at 0.35l. The blockage ratio is 1.6% for α = 30°. The value of V is 25.0-50.0±0.2 m/s and the Reynolds number based on l, Re_l, ranges from 6.68×10^4 to 3.98×10^5.

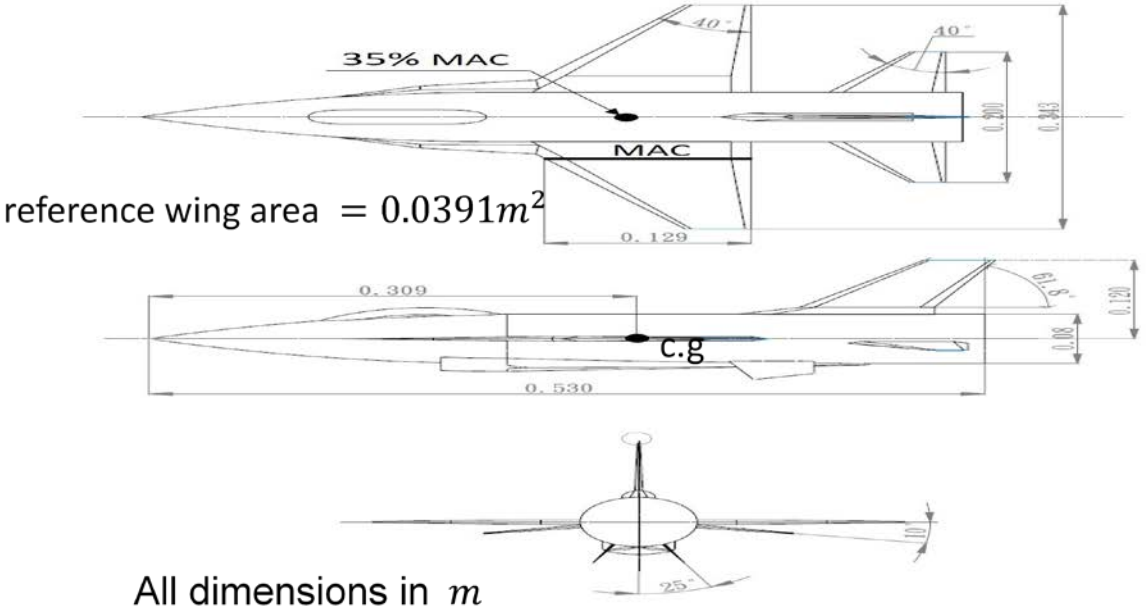

Figure 1 A standard dynamics model

2.2 Rotary balance

Rotary balance testing uses a model that rotates at a fixed value of Ω about an axis that is parallel to the freestream velocity vector. This study uses a five-component force balance (strain-gage type) to measure the normal force (NF, C_N), the side force (SF, C_Y), the rolling moment (RM, C_l), the yawing moment (YM, C_n) and the pitching moment (PM, C_m). The maximum loads for the force balance are shown in Table 1.

Static calibration was conducted to determine the sensitivity constants for each component and the interactions between all of the components. The uncertainty for each component is determined to be less than 0.5%. The balance was mounted to a C-shaped truss structure (arc length = 0.55 m and radius = 0.53 m), as shown in Fig. 2. Note that there are strong vortical flows for many fighter designs. The presence of the truss structure may result in premature vortex breakdown and affect the balance outputs. Taking structural vibrations and dynamic balancing into account [21], the mechanical design allows a value for α from 0° to 30° while keeping the same axis of rotation and the value of β is 0°. Both angles are constant during each rotational cycle. The rotary balance contains a bearing for the rotating arm (=

0.26 m) which is driven by a motor and a helical gear motor reducer (Varitron, GH28-750-3~25). An inverter (Delta Electronics, VFD7A5MS23ANSAA) controls the value of Ω up to 360 rpm (torque = 19 N-m). The value of κ ranges from -0.1 to 0.1 (Ω = 20-300 rpm). A 12-slip ring assembly transmits signals from the force balance and the WIKA amplifiers (EZE10X005003) are used to increase the signal-to-noise ratio. A data acquisition system (NI-9220, 16 channels) records the outputs at a sampling rate of 5 kHz.

Table 1 Maximum loads for the force balance

Component	Max load
Normal force, NF	311 N
Side force, SF	311 N
Rolling moment, RM	1.92 N-m
Yawing moment, YM	4.94 N-m
Pitching moment, PM	4.94 N-m

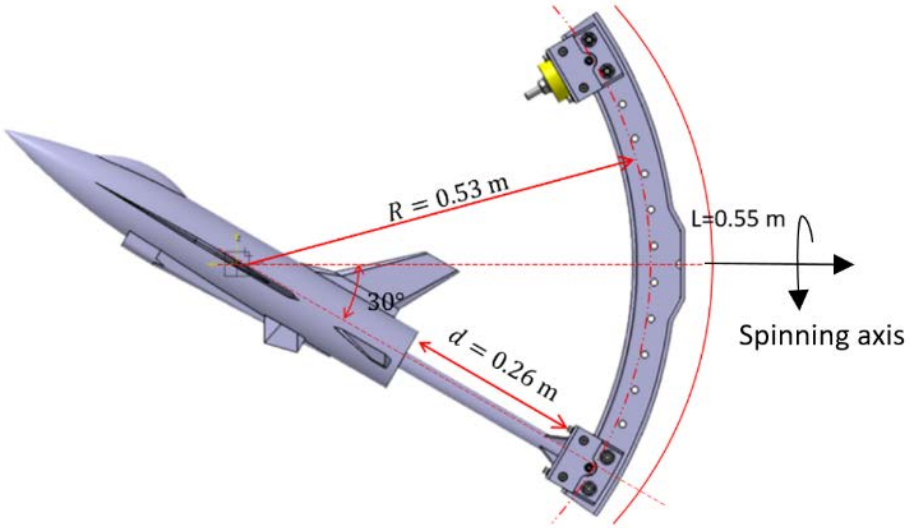

Figure 2 Test rig

2.3 Data processing

The forces and moments that act on a model in a spinning motion are gravitational, inertial and aerodynamic and vary with the attitude of the model and Ω. The sinusoidal variations (2 Hz) due to gravity (model weight) in the horizontal test setup are eliminated using a low-pass filter of 10 Hz. The inertial tares, F (forces and moments), that act on a model measured by rotating a model in the clockwise and counter-clockwise directions in a wind-off condition. 4th-order polynomial equations, $F = A_o+A_1\Omega+A_2\Omega^2+A_3\Omega^3+A_4\Omega^4$, for each value of α are determined to eliminate still-air damping in the wind-on condition. The aerodynamic data in a spinning motion is calculated by subtracting these inertial tares from the output from the force balance. The uncertainty in the output from the force balance is determined for three repeated runs at V = 50.0 m/s and α = 30°, as shown in Table 2. The correction to α due to sting deflection under steady loads is less than 0.1°.

Table 2 Uncertainty in balance outputs

C_N	C_y	C_l	C_m	C_n
0.009	0.009	0.008	0.004	0.007

To validate the performance of the rotary balance apparatus at the ASTRC, previous data from studies by Jermey and Schiff [22] and Huang et al. [23] for a SDM is used. The test conditions are shown in Table 3. The experiments at the ASTRC and FD-09 are in an incompressible flow regime. The respective value of Re_l is 6.68×10^4~3.98×10^5 and 8.8×10^5. The Mach number at NASA Ames is 0.6. The respective values of α and κ are 0°-30° and -0.1~0.1 for all three tests. The difference in aerodynamic coefficients (AC) for this study (V = 50 m/s, Re_l = 3.98×10^5), NASA Ames and FD-09, σ, are determined as below:

$$\sigma = \sqrt{\frac{1}{N-1}\sum_1^N (AC_{ASTRC} - AC)^2} \quad (1)$$

Table 3 Test conditions

	ASTRC	Ames	FD-09
tunnel, m^2	1.2×1.8	1.2×1.8	3×3
l, m	0.129	0.189	0.256
V, m/s	25-50 m/s	M = 0.6	50 m/s
Re_l	6.68×10^4~3.98×10^5	8.8×10^5	8.8×10^5
α	0°-30°	0°-30°	0°-30°
κ	-0.1~0.1	-0.1~0.1	-0.1~0.1

III. RESULTS AND DISCUSSION

3.1 Aerodynamic coefficients

The aerodynamics for an aircraft during a spin is dominated by a separated flow effect, which is sensitive to a change in the Reynolds number. The variation in the aerodynamic coefficients for α = 10° with κ is shown in Fig. 3. For a value of Re_l of 1.59~3.98×10^5, the value of C_N (= 0.587~0.682) increases as Re_l increases and the effect of κ is less significant (variation is less than 1%) (Fig. 3a). The results are approximately symmetrical with respect to the y-axis (positive and negative values of κ) for Re_l of 1.59×10^5. For a rotational symmetry with respect to the origin, the value of C_Y decreases as Re_l increases. An increase in Re_l results in a greater side force (Fig. 3b). The effect of Re_l on moments is most significant for C_m (Fig. 3c) and least significant for C_l (Fig. 3d). C_l and C_n (Fig. 3e) are an odd function of κ, which is in agreement with the results of Huang et al. [23].

For α = 30° (steep mode spinning motion) and Re_i = 6.68×10^4~3.98×10^5, the aerodynamic coefficients are shown in Fig. 4. The value of C_N is considerably greater than that for α = 10° and increases as Re_l increases. A change in κ results in a greater variation in C_N for any increase in Re_l. The effect of Re_l (= 1.59~3.98×10^5) on C_Y is not significant, except for Re_l = 6.68×10^4. For Re_l = 6.68×10^4~2.02×10^5, there is similar variation in C_m with κ and the value is greater for Re_l = 3.98×10^5. The variation in C_l with κ is opposite to that for α = 10°. An increase in κ results in a greater value of C_l. The effect of Re_l is also observed for greater value of κ. Re_l has the least effect on C_n.

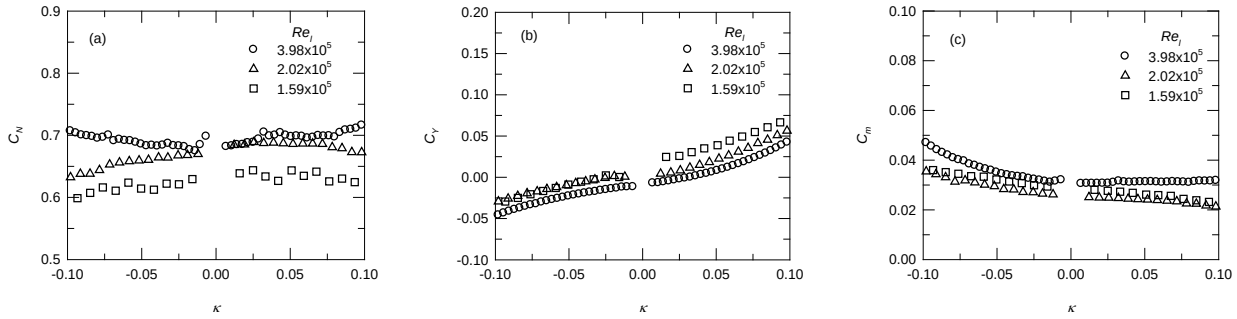

Normal force coefficient Side force coefficient Pitching moment coefficient

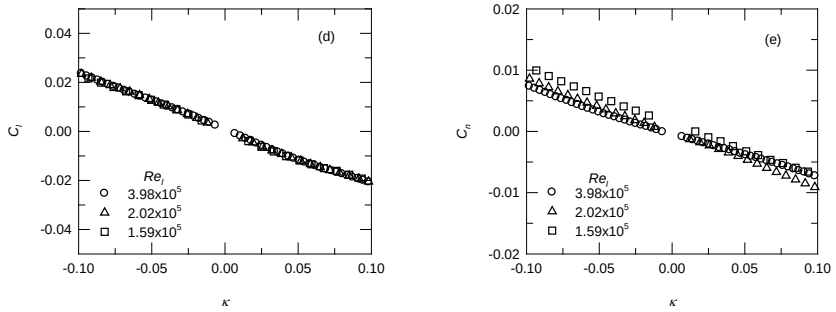

Rolling moment coefficient Yawing moment coefficient

Figure 3 The effect of Reynolds number on aerodynamic coefficients for α = 10°

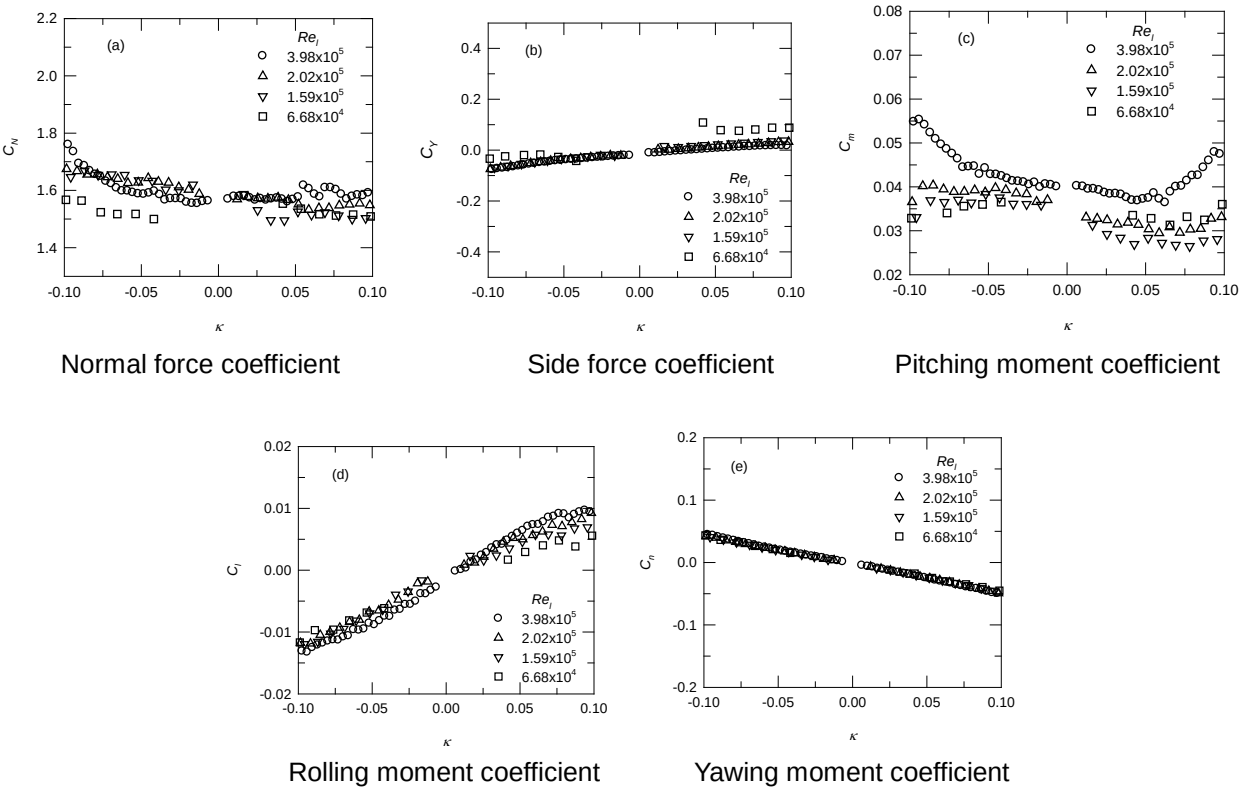

Figure 4 The effect of Reynolds number on aerodynamic coefficients for $\alpha = 30°$

3.2 Effect of Reynolds number and compressibility

For rotary balance tests at NASA Ames [22] and FD-09 [23], the value of Re_l is 8.8×10^5. The respective freestream speed is Mach 0.6 and 50 m/s. This study uses a value of V = 50 m/s and $Re_l = 3.98\times10^5$. The difference between FP-09 and ASTRC shows the effect of Re_l. Compressibility effect is determined in the NASA Ames's experiments. Huang et al. [23] showed that the blockage ratio and model support affect the measurement of C_m.

The variation in C_N with κ for $\alpha = 0°$-30° is shown in Fig. 5. For all three tests, C_N increases as α increases. This result agrees reasonably well with the results for NASA Ames and FD-09 at lower value of α, but not for α =30°. The difference is more significant at greater value of κ (FD-09), possibly because of the vibrational and structural characteristics of the apparatus and the tunnel support system [21]. In a steady spin, it implies zero accelerations. Fig. 6 shows the value of C_Y ($\approx \pm0.07$) is considerably lower than that of C_N ($\approx$ 0-1.8). Variation of C_Y with κ shows a similar trend for all three tests. The present results are less than those in NASA Ames and FD-09, but not for $\alpha = 0°$. The discrepancy is due to the difference in Re_l. The distribution for moments is shown in Figs. 7-9. The effect of Re_l and compressibility on C_l and C_n is less significant. This is not true for C_m for α = 20° and 30°. This may be due to the vortices generated by a test model which interact with a downstream support and affect pitching moment [21, 23]. The effect of a downstream support needs to be further studied.

The deviation in force coefficients between the present data, NASA Ames and FD-09, σ-C_N and σ-C_Y, is shown in Fig. 10. The solid symbol represents the deviation between the present and NASA Ames tests (the effect of Re_l and compressibility) while the hollow symbol is for FD-09 (the effect of Re_l). The figure shows that the value of σ-C_N increases as α increases. The effect of Reynolds number is more significant and dominated for greater α. For σ-C_Y, the value (= 0.002-0.028) is less than that for σ-C_N (=0.006-0.083). As shown in Table 2, the uncertainty for the outputs of C_N and C_Y is 0.009. This implies that the Reynolds number is the dominant factor on C_N and C_Y for $\alpha = 0°$-30°.

The deviation in moment coefficients (σ-C_m, σ-C_n and σ-C_l) is shown in Fig. 11. For σ-C_m, the effect of the Reynolds number and compressibility is more pronounced than that for σ-C_N. For σ-C_n and σ-C_l, the value is less than 0.005. Table 2 shows that the respective uncertainty for the outputs of C_n and C_l is 0.007 and 0.008 so the Reynolds number and compressibility have only a minor effect on the yawing and rolling moments in a steady spin.

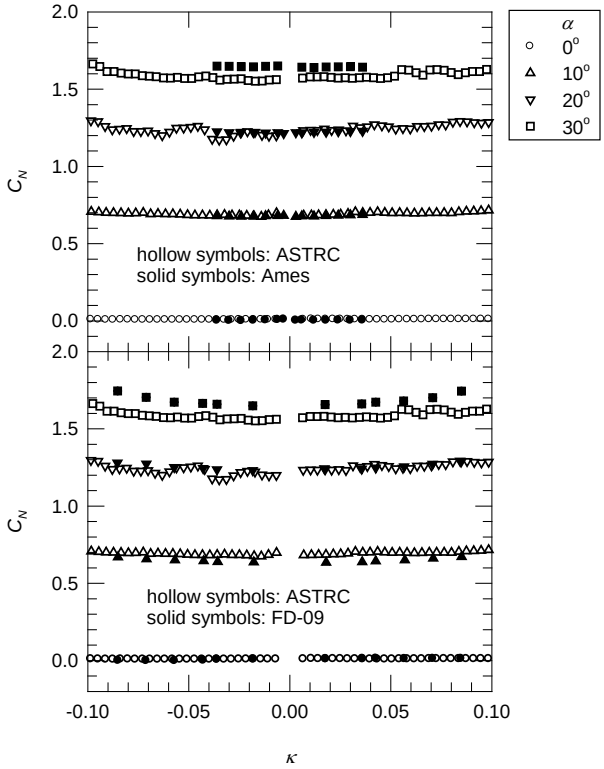

Figure 5 Normal force coefficient

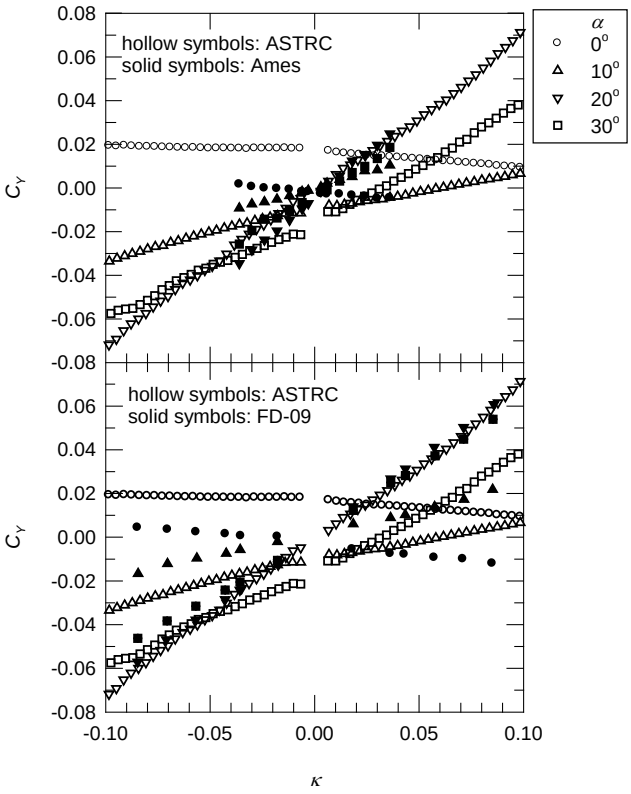

Figure 6 Side force coefficient

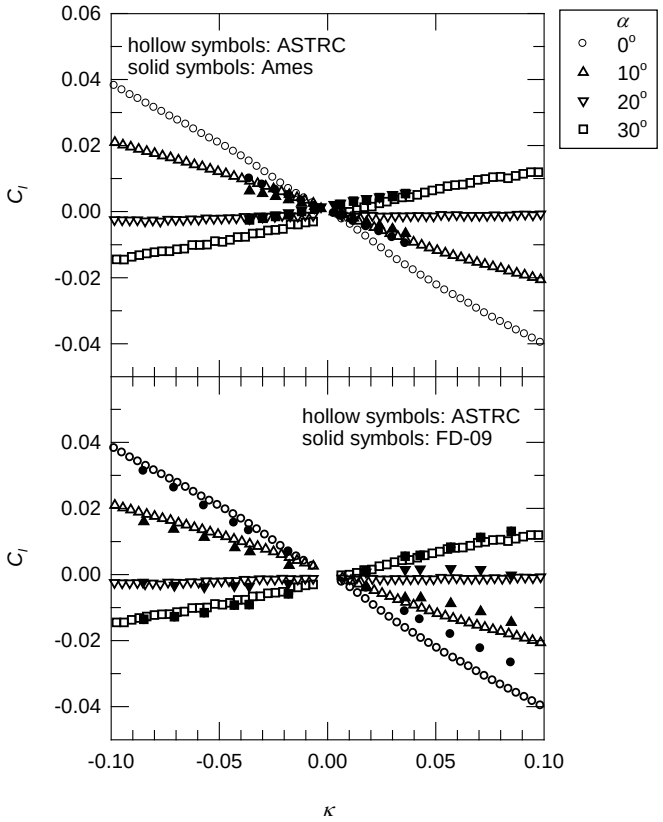

Figure 7 Rolling moment coefficient

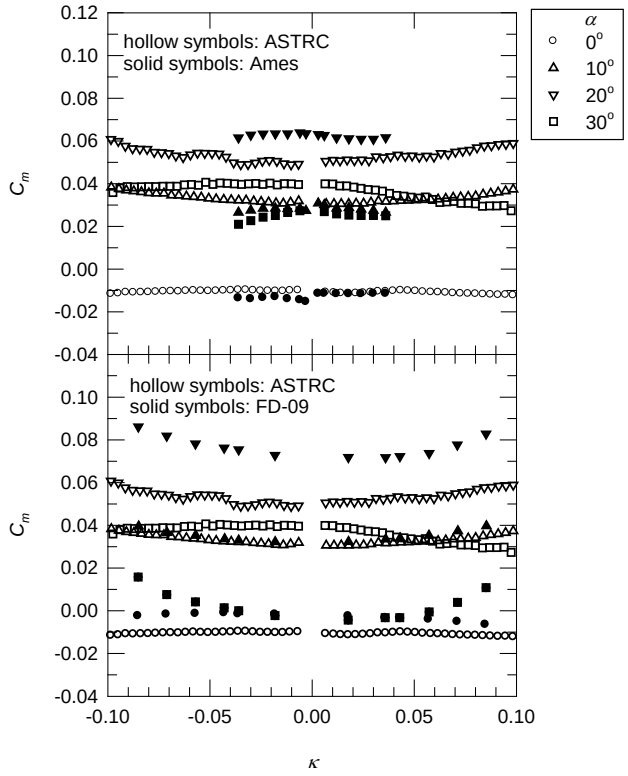

Figure 8 Pitching moment coefficient

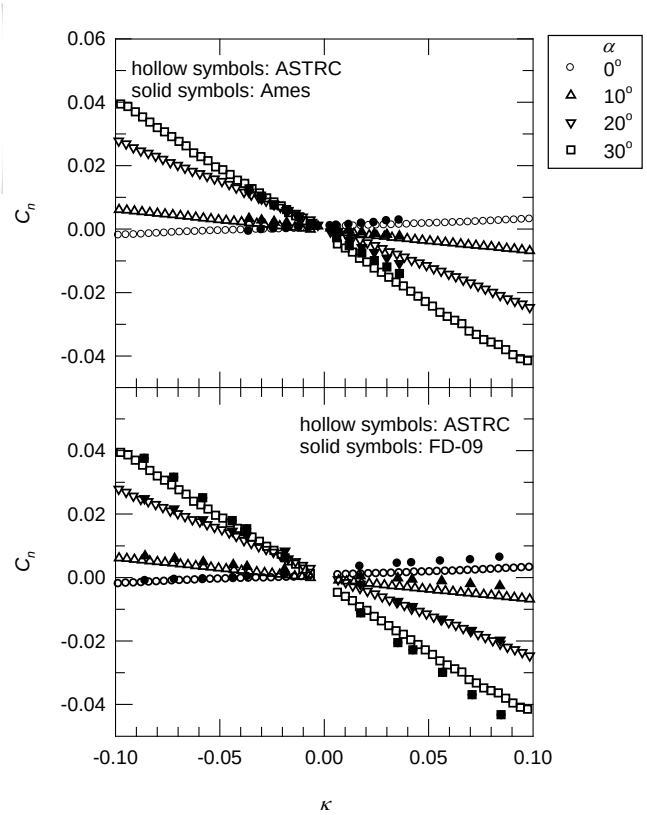

Figure 9 Yawing moment coefficient

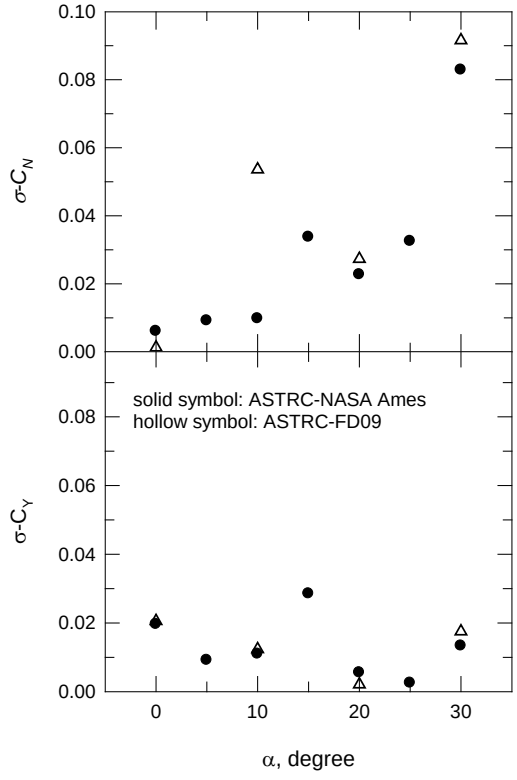

Figure 10 Deviation in force coefficients

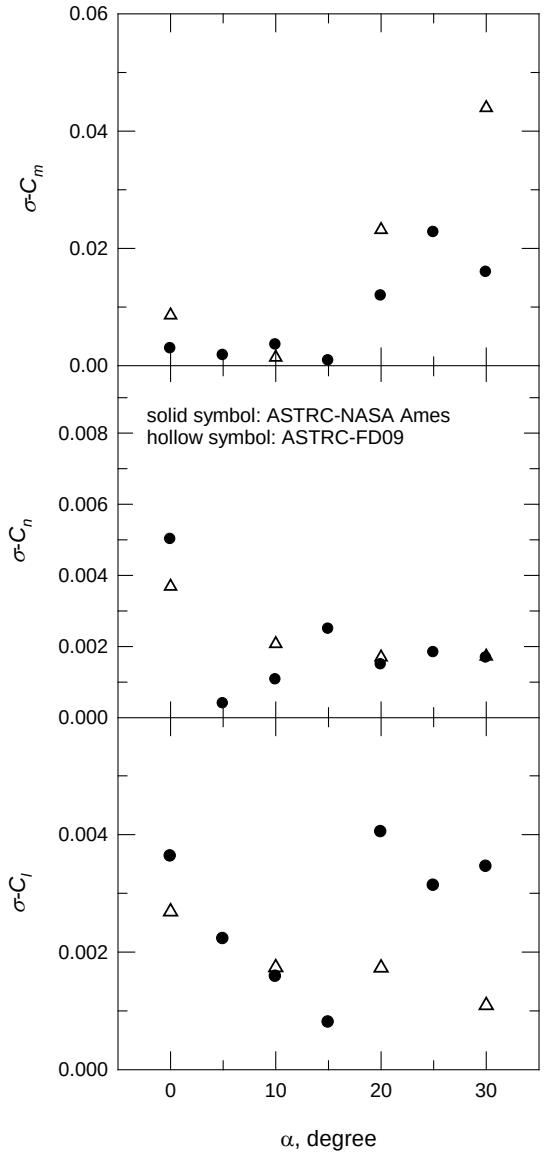

Figure 11 Deviation in moment coefficients

3.3 Aerodynamic derivatives

The derivative of forces and moments with respect to a change in Ω for a specific value of α determines the changes in aerodynamic coefficients in a spin. A comparison of the results for this study and NASA Ames is presented. Fig. 5 shows that there is a minor variation in the value of C_N for a specific value of α. Fig. 12a shows that there is no relationship between $C_{N\Omega}$ and α for either test. The value of $C_{Y\Omega}$ increases for α = 0°-20° and decreases for greater values of α, as shown in Fig. 12b. There is good agreement between results for the two tests. In terms of the derivative of the moment coefficients, Fig. 13a shows that there is a minor variation in $C_{m\Omega}$ with respect to α so there is minor variation in C_m for a specific value of α. An increase in the value of Ω results in a decrease in the value of C_n. The perturbation in Ω has a greater effect on the value of $C_{n\Omega}$ as α increases, as shown in Fig. 13b. Fig. 13c shows that the effect on $C_{l\Omega}$. The value of $C_{n\Omega}$ increases for greater α. There is good agreement in terms of the values of $C_{n\Omega}$ and $C_{l\Omega}$ so the flow for greater α in a spin is dominated by roll and yaw motions.

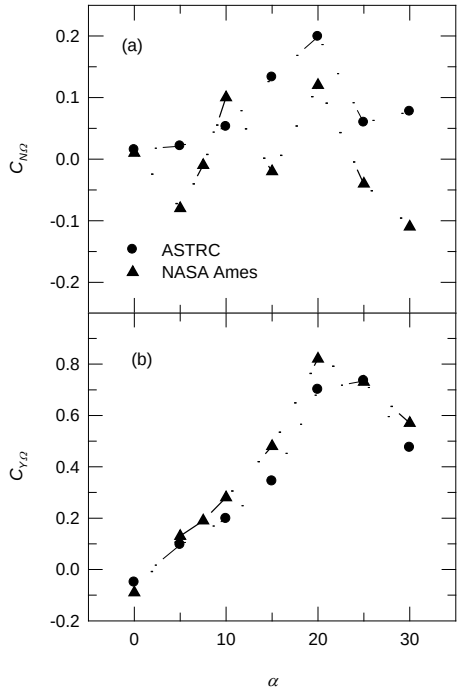

Figure 12 Derivative of force coefficients

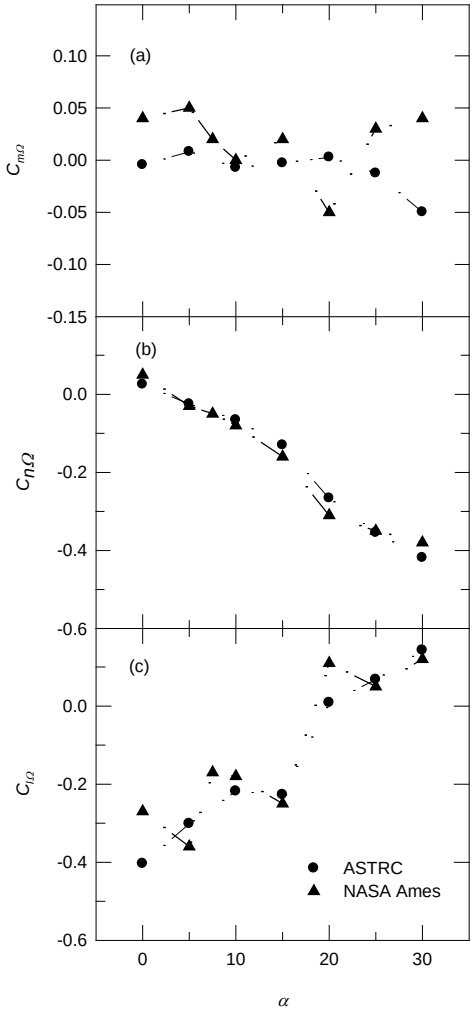

Figure 13 Derivative of moment coefficients

IV. CONCLUSIONS

Spinning or coning endangers all types of aircraft. This study develops a rotary balance apparatus. The measurements use a 5-component force balance to determine the aerodynamic coefficients for a SDM. The Reynolds number has the most significant effect on the coefficients for normal force and pitching moment. The results are compared with those for tests in NASA Ames (the effect of Reynolds number and compressibility) and FD-09 (the effect of Reynolds number). The difference in the coefficients for normal force and pitching moment increase as the angle of attack increases, mainly due to the effect of the Reynolds number. Future studies for a SDM with greater mean aerodynamic chord or freestream velocity (an increase in Reynolds number) are required.

In terms of the coefficients of side force and yawing/rolling moments, there is good agreement so the Reynolds number and compressibility have a minor effect. The perturbation in yawing and rolling moments with respect to spin frequency increases as the angle of attack increases. The aerodynamic derivative with respect to the spin frequency is approximately the same so the flow in a spin is dominated by yaw and rolling motions.

ACKNOWLEDGMENTS

The authors acknowledge the financial support of the National Chung-Shan Institute of Science and Technology (XW07027P079-CS).

NOMENCLATURE

b	wing span
C_N	normal force coefficient
C_Y	side force coefficient
$C_{Y\Omega}$	side force derivative
C_l	rolling moment coefficient
$C_{l\Omega}$	rolling moment derivative
C_m	pitching moment coefficient
C_n	yawing moment coefficient
$C_{n\Omega}$	yawing moment derivative
l	mean aerodynamic chord
Re_l	Reynolds number based on mean aerodynamic chord
V	freestream velocity
α	angle of attack
β	sideslip angle
κ	reduced frequency
Ω	spin frequency

REFERENCES

[1] Bennett CJ, Lawson NJ, "On the Development of Flight-Test Equipment in Relation to the Aircraft Spin," *Progress in Aerospace Sciences*, Vol. 102, 2018, pp. 47-59.

[2] Burk SM Jr., Bowman JS Jr., White WL, "Spin-Tunnel Investigation of the Spinning Characteristics of Typical Single-Engine General Aviation Airplane Designs. 2: Low-Wing Model A; Tail Parachute Diameter and Canopy Distance for Emergency Spin Recovery," NASA TP-1076, 1977.

[3] Bihrle W Jr., Barnhart B, "Spin Prediction Techniques," *Journal of Aircraft*, Vol. 20, No. 2, 1983, pp. 97-101.

[4] Ericsson LE, Beyers ME, "Flat Spin of Axisymmetric Bodies," *Journal of Aircraft*, Vol. 32, No. 6, 1995, pp. 1205-1212.

[5] Malik B, Akhtar S, Masud J, "Dynamic Analysis and Nonlinear Simulation of Aircraft Flat Spin," *Journal of the Chinese Institute of Engineers*, Vol. 40, No. 6, 2017, pp. 471-481.

[6] Sidoryuk ME, Khrabrov AN, "Estimation of Regions of Attraction of Aircraft Spin Modes," *Journal of Aircraft*, Vol. 56, No. 1, 2019, pp. 205-216.

[7] Farcy D, Khrabrov AN, Sidoryuk, ME, "Sensitivity of Spin Parameters to Uncertainties of the Aircraft Aerodynamic Model," *Journal of Aircraft*, Vol. 57, No. 5, 2020, pp. 922-937.

[8] Anglin EL, "Aerodynamic Characteristics of Fighter Configurations during Spin Entries and Developed Spins," *Journal of Aircraft*, Vol. 15, No. 11, 1978, pp. 769-776.

[9] Murch AM, "Aerodynamic Modeling of Post-Stall and Spin Dynamics of Large Transport Airplane," Mater Thesis, Department of Aerospace Engineering, Georgia Institute of Technology, USA, 2007.

[10] Malik B, Akhtar S, Masood J, "Analysis of Spin Characteristics of a High Performance Aircraft with High Alpha Yawing Moment Asymmetry," AIAA Paper 2016-1038, AIAA SciTech, San Diego, California, USA, 4-8 January, 2016.

[11] Khrabrov A, Sidoryuk M, Goman M, "Aerodynamic Model Development and Simulation of Airplane Spin and Upset Recovery," Progress in Flight Physics, Vol. 5, 2013, pp. 621-636.

[12] Stone RW Jr., Burk SM Jr., Bihrle W Jr., "The Aerodynamic Forces and Moments on a 1/10 Scale Model OF a Fighter Airplane in Spinning Attitudes as Measured on a Rotary Balance in the Langley 20-Foot Free-Spinning Tunnel," National Advisory Committee for Aeronautics, Technical Note 2l8l, September 1950.

[13] Bowman JS, "Summary of Spin Technology as Related to Light General-Aviation Airplanes," NASA Technical note D6575, December, 1971.

[14] Malcolm GN, "New Rotation-Balance Apparatus for Measuring Airplane Spin Aerodynamics in the

Wind Tunnel," *Journal of Aircraft*, Vol. 16, No. 4, 1979, pp. 264-268.

[15] Malcolm GN, Schiff LB, "Recent Developments in Rotary-Balance Testing of Fighter Aircraft Configurations at NASA Ames Research Center," NASA Technical Memorandum 86714, July, 1985.

[16] Malcolm GN, Kramer BR, Suhrez CJ, Ayers BF, James KD, O'leary C, Wier B, Walker JM, "USNK Rotary-Balance Test Comparisons With A Generic Fighter Mode," AIAA Paper 94-0196, 32nd Aerospace Sciences Meeting & Exhibit, Reno, NV, USA, January 10-13, 1994.

[17] Du XQ, Hao WD, Chen B, "Summary of the Dynamic Test Capabilities at CARIA Low Speed Wind Tunnel," 25th International Congress of the Aeronautical Sciences, 2006.

[18] Murch AM, Foster JV, "Recent NASA Research on Aerodynamic Modeling of Post-Stall and Spin Dynamics of Large Transport Airplanes," AIAA Paper 2007-463. 45th AIAA Aerospace Sciences Meeting and Exhibit, Jan 8-11, 2007. Reno, USA.

[19] Denham C, Owens DB, "Rotary Balance Wind Tunnel Testing for the FASER Flight Research Aircraft," AIAA Paper 2016-3105, AIAA Atmospheric Flight Mechanics conference, Washington DC, USA, 13-17 June, 2016.

[20] Ragheb AM, Selig MS, "Wind Tunnel Testing of Wings in Spin," AIAA Paper 2016-1073, AIAA SciTech, San Diego, California, USA, 4-8 January, 2016.

[21] Fluid Dynamics Panel working group 11, "Rotary-Balance Testing for Aircraft Dynamics," AGARD Advisory Report No. 265, North Atlantic Treaty Organization December, 1990.

[22] Jermey C, Schiff LB, "Aerodynamic Characteristics of the Standard Dynamics Model in Coning Motion at Mach 0.6," NASA Technical Memorandum 86717, July, 1985.

[23] Huang H, Zhang YS, Liu D, "Rotary Balance Apparatus in FD09 Wind Tunnel," *Advances in Aeronautical Science and Engineering*, Vol. 5, No. 4, 2014, pp. 429-434.

[24] Beyers ME, Moulton BE, "Stability Derivatives due to Oscillations in Roll for the Standard Dynamics Model at Mach 0.6," Report LTR-UA-64, National Aeronautical Establishment, Canada, Jan. 1983.